Coral Reefs (2001) 20: 361–372
DOI 10.1007/s00338-001-0193-6

REPORT

P. Douillet · S. Ouillon · E. Cordier

A numerical model for fine suspended sediment transport in the southwest lagoon of New Caledonia

Received: 3 February 2001 / Accepted: 6 July 2001 / Published online: 25 October 2001

Abstract A hydrodynamic-transport coupled model is used to understand the transport of fine suspended sediments in the southwest lagoon of New Caledonia. The hydrodynamic model is briefly presented and the circulation due to the tide and to averaged trade wind forcings is analyzed. The transport model for fine suspended sediment is described. Parameters involved in this model (settling velocity, critical shear stresses, erosion rate coefficient, Schmidt number) are discussed and a calibration procedure is proposed. Using the resultant parameters, the erosion and deposition areas predicted by the sediment-transport model are in very good agreement with the distribution of the percentage of mud at the seabed. The sensitivity of the model to the different sedimentary parameters is studied, and the influences of the tide and wind on deposition and erosion are discussed. The influence of the wind is dominant in seabed exchange processes in shallow areas and produces large erosion rates where the water depth is less than 20 m. The tide controls the particulate transport, vertical mixing, and deposition rates in the areas where the influence of the wind is weak.

Keywords Lagoon · Coastal hydrodynamics · Sediment transport · Numerical model · Deposition · Erosion · New Caledonia

Introduction

In New Caledonia, where open-cast mining plays a significant economic role, the sediment distribution and dynamics in the lagoon are of primary importance for the biogeochemical mechanisms of the coral reef lagoon ecosystems. Since 1996, a study of the anthropogenic and terrigenous input influence in the lagoon has been supported by the Institut de Recherche pour le Développement (IRD – formerly called ORSTOM) through the ECOTROPE program, which became a part of the French National Programme of Coastal Environment (PNEC) in 1999. The present paper presents part 1 of an ongoing investigation into the sediment dynamics of the southwest lagoon of New Caledonia.

The lagoons of New Caledonia, located 1,500 km east of Australia, are extensive, covering a total area of 24,000 km^2. The southwest lagoon is funnel shaped (Fig. 1) and has a mean depth of approximately 17.5 m. Its longest axis is 100 km and runs from northwest to southeast. Its width tapers from 40 km in the southeast to about 5 km in the northwest. Deep passes bisect the barrier reef and the reef crest is exposed at low tide.

Modeling can be used to describe and study the transport of suspended sediment. A hydrodynamic model is required to provide fields of velocity, bottom shear stress, and eddy viscosity for use in the sediment-transport model. Suspended sediment transport models have been mainly developed for rivers, flumes and coastal zones for non-cohesive particles (e.g., Celik and Rodi 1988; van Rijn et al. 1990; Ouillon and Le Guennec 1996; Chapalain and Thais 2000), in turbid estuaries for cohesive particles (e.g., Nicholson and O'Connor 1986; Teisson 1991; Brenon and Le Hir 1999), around sand beaches (e.g., Soulsby 1997), and in river plumes (e.g., Lin and Falconer 1996; Durand et al. 2001). Although several numerical models have been applied to the study of coastal lagoon hydrodynamics using one-dimensional (1D) models (Smith 1985), 2D models (Frith and Mason 1986; Prager 1991; Kraines et al. 1998), or 3D models (Tartinville et al. 1997), no suspended sediment transport model has yet been applied to coral reef lagoons.

The first part of the paper presents the field measurement strategy and the hydrodynamic model. The computed circulation due to the tide and wind forcings is analyzed in some detail since the lagoon hydrodynamics

P. Douillet (✉)
Centre IRD Nouméa, BP A5, 98848 Nouméa, New Caledonia
E-mail: douillet@noumea.ird.nc
Tel.: +687-260746
Fax: +687-264326

S. Ouillon · E. Cordier
LSEET/CNRS, Université de Toulon et du Var,
BP 132, 83957 La Garde cedex, France

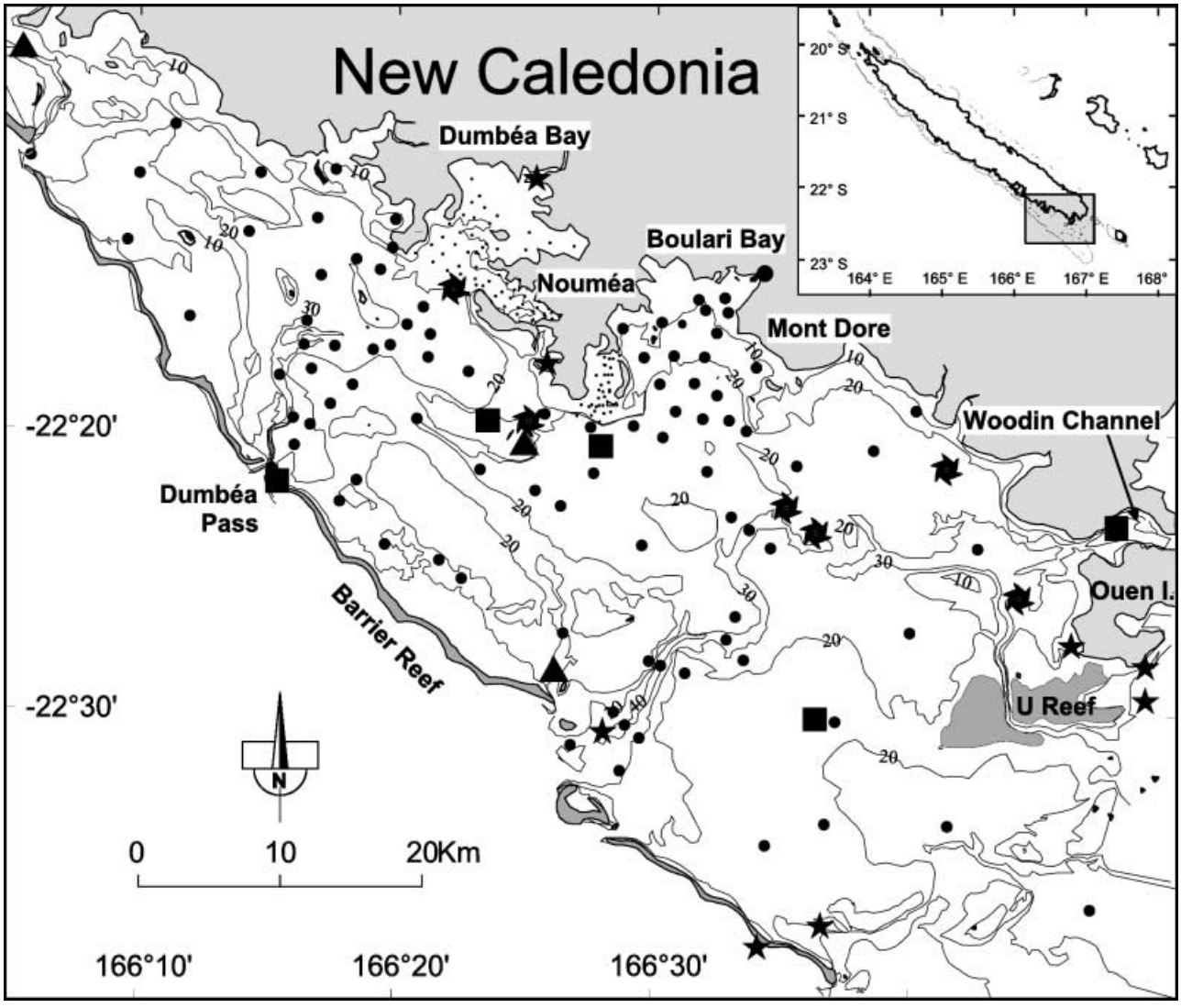

Fig. 1 The southwest lagoon of New Caledonia. Location of current-meter stations (■), meteorological stations (▲), tide gauges (★), CTD profiles (●), and ADCP stations (✸). Contours of water depths are in meters

drive the sediment dynamics as well as the bottom exchange. The suspended sediment transport model is described in the second part of the paper, and finally the model results are presented and discussed. A process for the calibration of the model parameters is proposed, and the sensitivity of the model to the different sedimentary parameters is studied. Using the derived set of parameters, the respective influences of tide and wind on deposition and erosion are discussed.

Field setting

In-situ data

Earlier hydrodynamic studies of the southwest lagoon showed that wind and tidal forces are the main mechanisms driving lagoon circulation (Jarrige et al. 1975; Morlière and Crémoux 1981; Morlière 1985). In order to develop a circulation model of the lagoon:

1. Further data were collected during cruises between 1988 to 1990 (Douillet et al. 1989, 1990);
2. Sea-level variations were measured using Aanderaa WLR7 tide gauges;
3. Wind was recorded continuously at different locations in the lagoon;
4. Aanderaa RCM9 current meters were moored at several places (Fig. 1);
5. Twenty two cruises have been dedicated since 1997 to determining the distribution of the hydrological parameters by running vertical profiles using a SeaBird SBE 19 CTD equipped with an additional Seapoint turbidity sensor;
6. Over the same period, an ADCP current meter (RDI WorkHorse 300 kHz) was moored at various stations, usually for approximately 1 month, to obtain information about the vertical structure of the current;

7. To complement the turbidity profile measurements, we used the available sedimentological studies of the lagoon (Debenay 1987; Chardy et al. 1988) for calibration and validation of the sediment transport model.

Description of the hydrodynamic model

The equations of the hydrodynamic model use the Boussinesq and hydrostatic approximations (e.g., Nihoul 1984; Blumberg and Mellor 1987; Ruddick et al. 1995). The vertical eddy viscosity is expressed using a mixing length formula. In order to maintain a uniform number of vertical grid points, the hydrodynamic equations are solved in σ-coordinates system (Blumberg and Mellor 1987; Hearn and Holloway 1990; Lazure and Salomon 1991; Deleersnijder and Beckers 1992). The solution of the hydrodynamic equations is based on the separation of the external and internal modes into two models which are computed simultaneously: a 2D model calculates the free surface elevations and supplies these to a 3D model. The model resolution is based on the alternating direction-implicit method (ADI; Leendertse 1967) for time discretisation, and on the finite difference method for space discretisation. It includes automatic treatment of wetting and drying (Lazure and Salomon 1991). The horizontal grid size is 500 m, and each water column is divided into 10 σ-levels. The integration time step is 10 min.

Hydrodynamic model results and circulation analysis

The two major factors controlling lagoon circulation in the southwest lagoon of New Caledonia are the tide and the wind (Douillet et al. 1989, 1990; Douillet 1998). The currents due to these forcing functions are calculated using the 3D model.

M_2 the lunar semidiurnal constituent, is the major constituent of the tide (Douillet 1998). The currents due to M_2 are low in magnitude (Fig. 2), peaking at 0.20 m s^{-1}. In the southern part of the lagoon, the tidal streams tend to align themselves along the lagoonal axis near the barrier reef and go around U Reef. The amplitude of this tidal current decreases from south to north, and the current is weaker north westward of Ouen Island where the lagoon is the deepest. On the west side of this island, the direction of the major axis of the currents turns, due to the presence of a reef near Ouen Island. In the passes, the current is generally strong and almost rectilinear. The tidal ellipses tend to become circular inside the lagoon and near the passes. This phenomenon may be linked to the presence of very deep riverbeds, which extend from the coast to the passes. The acceleration of the current was measured near Nouméa (Douillet 1998) and shown to be due to the presence of a channel which is shallower than in the northern or southern areas (Fig. 1).

The most frequently encountered wind regime in New Caledonia is the southeasterly trade wind (average speed 8 m s^{-1}, and direction 110°). The direction of current in the surface layer is totally governed by the wind direction and constrained by the boundaries of the lagoon (Fig. 3a). Spatial variations of the velocity modulus are slight. However, lower velocities may be observed in the canyons which lead to the passes along the coast, and in a deep area to the north of Ouen Island (depth over 30 m; see Fig. 1 for the positions of the canyons). In the

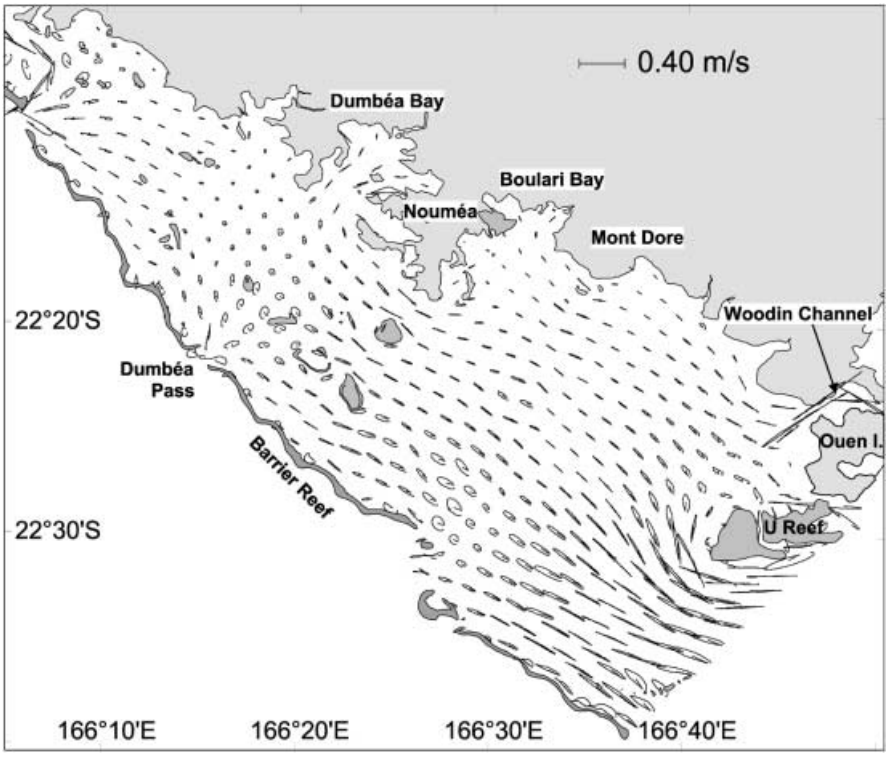

Fig. 2 Model simulation of the M_2 constituent: the ellipses of tidal currents

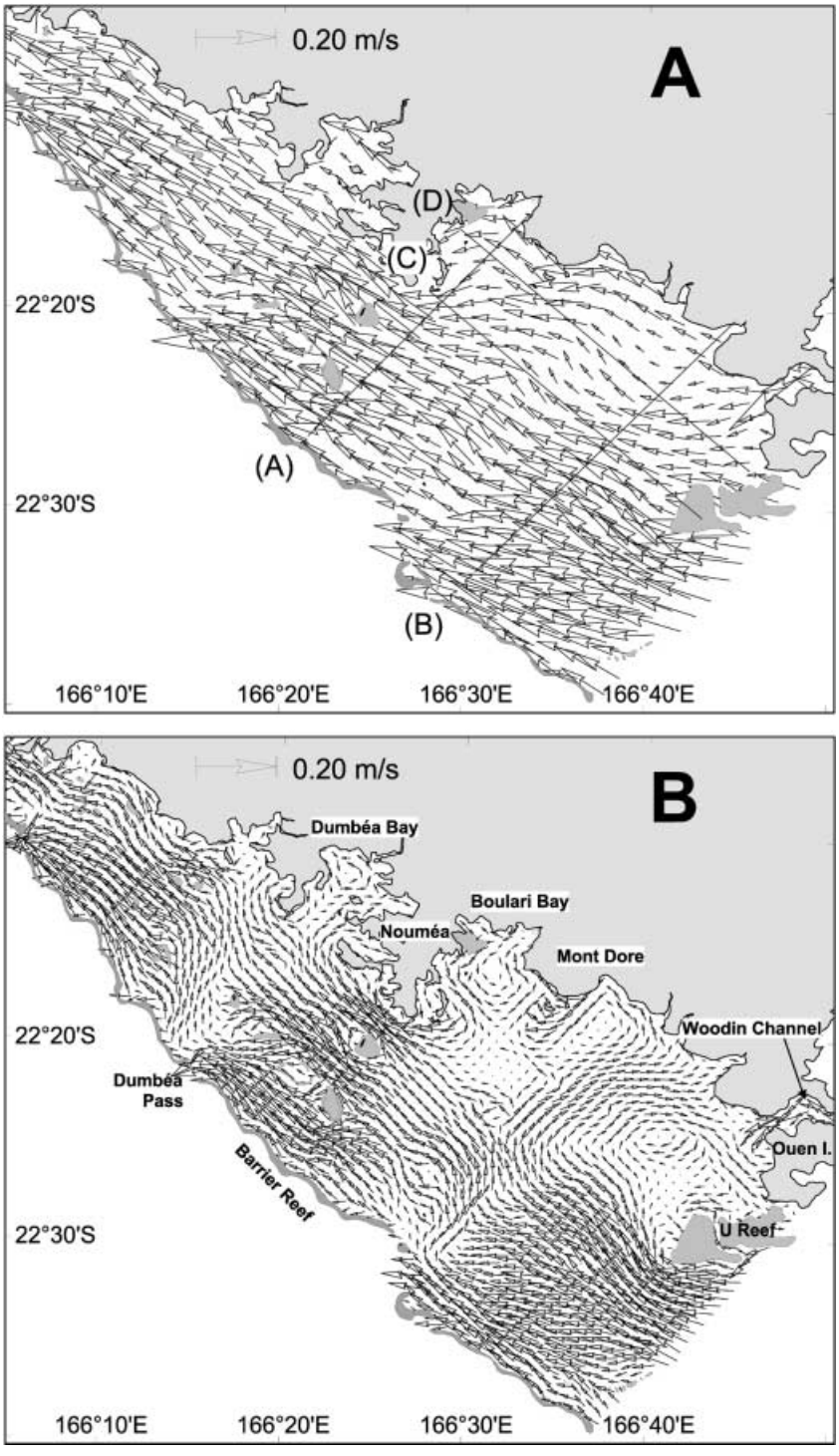

Fig. 3A,B Currents simulated by the model, generated by a southeasterly (110°) trade wind of 8 m s^{-1}. **A** Surface currents (only one out of two velocity vectors is plotted). **B** Bottom currents

deepest layer of the model, next to the bottom, the currents are far more complex (Fig. 3b). In the southeastern part, between U Reef and the barrier reef, the current is relatively strong. It flows in the same direction as the surface current, with a slight deviation in the bottom Ekman layer. There is a permanent vortex north of Ouen Island. This vortex is surrounded by the coast to the east, and by Ouen Island and U Reef to the south. There is only a small water inflow, in the southeast through Woodin Channel between the coast and Ouen Island. As the wind blows from the southeast, it pushes the surface water northwestwards, creating a slope of the sea surface. The model shows that the sea level is lower in the southeast than anywhere else in the lagoon. Thus, to balance the pressure gradient, a subsurface return current develops along the coast, feeding the bottom vortex observed north of Ouen Island. The gyre is approximately 20 km wide in the east-west direction, and

15 km in the south-north direction. Gyres also develop in the bay surrounding Nouméa, in Boulari Bay to the south, and in Dumbéa Bay to the north. The model, when forced by the wind only, clearly shows the role played by passes in emptying the lagoon (Fig. 3b).

The vertical structure of the current is presented in Fig. 4 (see the location of the cross sections on Fig. 3a). The cross section which goes from Boulari Bay to the barrier reef (Fig. 4a) shows the Boulari Bay vortex with a northwestward velocity component along the coast and a southeastward component at 22 km. This southeastward component is stronger at the bottom of the lagoon (0.04 m s^{-1}), and weakens toward the surface where it becomes negative at a depth of approximately 2 m. The cross section to the north of Ouen Island (Fig. 4b), which stretches from the coast to the barrier reef, shows a return southeastward current very close to the coast, already shown on the map of the lagoon bottom currents (Fig. 3b) and which reaches a maximum velocity of 0.03 m s^{-1}. It extends over a width of 8 km from the coast and a height of 25 m above the bed. The cross sections shown in Fig. 4c–d, lying parallel to the coast between Nouméa and Ouen Island, show the magnitude of the water mass coming from the south, which flows in the subsurface layer towards the coast at 90° to the main wind direction. This stream current is 9 km in width and extends from the surface to the lagoon floor. It feeds partly into the vortex to the north of Ouen Island.

Description of the suspended sediment transport model

The suspended sediment transport is modeled by an equation expressing the local variation of the particle concentration due to the advective motion and turbulent diffusion of surrounding sediment. The advection of particles results from the addition of the local velocity and their fall velocity under gravity. Whereas the general advection-diffusion equation is the same for sand and for mud, the boundary conditions are different for cohesive and non-cohesive particles. More detailed descriptions of the physical processes involved in the transport into suspension of fine sediments may be found in Mehta et al. (1989), and Teisson et al. (1993). The equation for the suspended particulate matter concentration (hereafter denoted C) is then:

$$\frac{\partial C}{\partial t}+\frac{\partial (uC)}{\partial x}+\frac{\partial (vC)}{\partial y}+\frac{\partial [(w-W_s)C]}{\partial z} = \frac{\partial}{\partial x}\left(K_h\frac{\partial C}{\partial x}\right)+\frac{\partial}{\partial y}\left(K_h\frac{\partial C}{\partial y}\right)+\frac{\partial}{\partial z}\left(K_z\frac{\partial C}{\partial z}\right) \quad (1)$$

where u, v, and w are the velocity components, W_s is the settling velocity of particles, and K_h and K_z are the horizontal and vertical eddy diffusivities of particles, respectively.

For a given type of particles, the settling velocity may be either measured or derived from Stokes' formula for particles with a diameter less than 100 μm as follows:

$$W_s=\frac{(s-1)\,g\,D_s^2}{18\,v} \quad (2)$$

where D_s is the representative diameter of the particles, s is the ratio of densities of particle and water, i.e., $s=\left(\frac{\rho_{particle}}{\rho_{water}}\right)$, v is the kinematic molecular viscosity of water, and g is the acceleration due to gravity. In the southwest lagoon of New Caledonia, measurements made in Dumbéa Bay, north of Nouméa, showed that the non-flocculated mud particles in suspension have a representative diameter of 7 μm (O'Callaghan 1999). This value, which is the one used in the simulations, provides a settling velocity of 4.4×10^{-5} m s^{-1}.

The vertical eddy diffusivity of particles, K_z, is generally considered to be proportional to the vertical eddy viscosity N_z according to:

$$K_z=\frac{N_z}{\sigma_c} \quad (3)$$

where σ_c is the Schmidt number, which assumes that the mass turbulent transfer is similar to momentum. However, experimental work showed that the hypothesis that the K_z profiles are proportional to the N_z profiles leads to unrealistic, and excessively low, diffusivity below the surface in the absence of wind (Coleman 1970). Consequently, van Rijn (1986) suggested considering a constant vertical diffusivity in the upper part of the water column. In this work, we chose to consider K_z as a constant between the surface and the depth where N_z is maximum. This choice leads to a non-zero concentration at the sea surface.

The boundary conditions need particular attention. Where lateral boundaries are open, a Neumann condition is imposed in the case of an outgoing flux:

$$\frac{\partial C}{\partial x_i}=0 \quad x_i=x,y \quad (4)$$

and a value of concentration is imposed in the case of an inflow flux.

At the sea surface, the condition is that there is no exchange of particles through the surface, i.e.,

$$\left(K_z\frac{\partial C}{\partial z}-W_sC\right)_{surface}=0 \quad (5)$$

At the bottom, the boundary condition is that the fluxes of particles between the water column and the seafloor is as follows:

$$\left(K_z\frac{\partial C}{\partial z}-W_sC\right)_{bottom}=D-E \quad (6)$$

where D and E are the exchange rates of particles through deposition and erosion, respectively.

For a given fine sediment, the deposition rate is proportional to the concentration near the bottom and to the settling velocity. In Krone's (1962) widely used formula, the deposition rate depends also on the bed shear

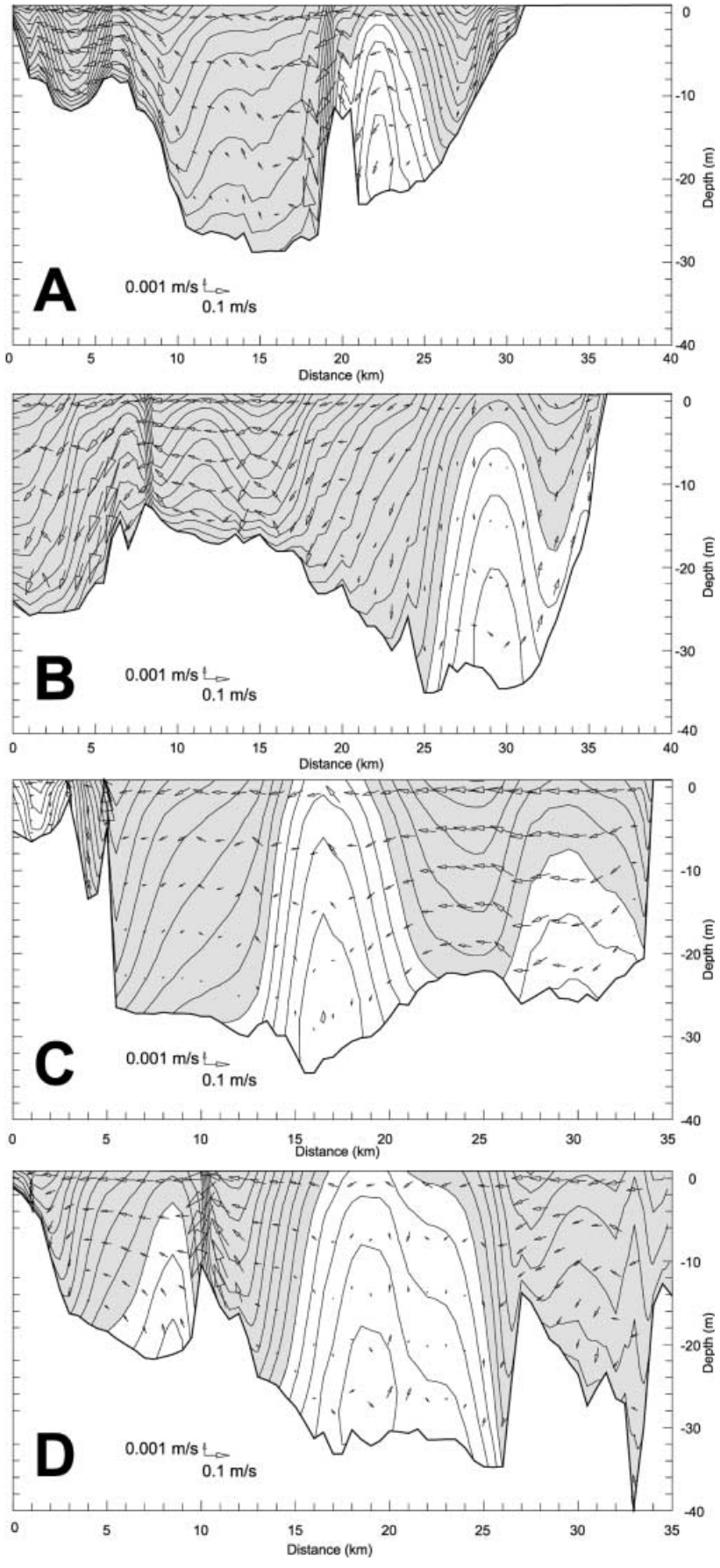

Fig. 4A–D Vertical current cross sections for a southeasterly (110°) trade wind of 8 m s^{-1}. The isotachs represent the component of the velocity perpendicular to the cross section (every 0.01 m s^{-1}), and the *shaded* region corresponds to negative values of this component (northeastward for **A** and **B**, east-southward for **C** and **D**). The *arrows* represent the along-section and vertical components of velocity. Locations of cross sections **A**, **B**, **C**, and **D** are shown in Fig. 3a

stress as compared to a critical shear stress for deposition which is specific to the type of particles considered:

$$D = W_s C\left(1 - \frac{\tau}{\tau_{cd}}\right) \text{ for } \tau < \tau_{cd} \text{ and } D = 0 \text{ for } \tau > \tau_{cd} \quad (7)$$

where D is expressed in kg m^{-2}s^{-1}, τ is the bed shear stress in N m^{-2}, and τ_{cd} is the critical shear stress for deposition.

The erosion rate depends on the nature of the deposit and on the excess of bed shear stress as compared to a threshold value. Over consolidated bottoms, it gives (Partheniades 1965) E, being expressed in kg m^{-2} s^{-1},

$$E = ke\left(\frac{\tau}{\tau_{ce}} - 1\right) \text{ for } \tau > \tau_{ce} \text{ and } E = 0 \text{ for } \tau < \tau_{ce} \quad (8)$$

where τ_{ce} is the critical shear stress for erosion, and ke is the erosion rate coefficient depending on the soil consolidation. In our preliminary study, we assume that the erosion rate coefficient in the southwest lagoon is proportional to the local percentage of mud at the seabed, hereafter denoted P_{mud}, according to:

$$ke = ke_c P_{mud} \quad (9)$$

where ke_c is a fitting parameter. An averaged value of ke_c is considered in this study and is applied to the entire lagoon, except over the reef bottom which is generally not supplied with fine sediments and where, consequently, erosion does not occur.

Model results and discussion

Determination of the critical shear stresses for deposition and erosion

One difficulty in modeling fine sediment transport is finding the critical shear stresses for deposition and erosion (τ_{cd} and τ_{ce}, respectively), and the erosion rate coefficient (ke). These parameters can be measured in a flume under controlled flow conditions (e.g., Piedra-Cueva et al. 1997), and such a method is particularly suitable for homogeneous sediments. The parameters can also be chosen so as to provide the best agreement between model results and observations. In the latter case, the resulting values of these parameters can be compared to those cited in the literature. However, published values generally refer to muddy estuaries and their ranges are very wide. For example, Le Normant (1995) and Schaaf (1999) quote estimates of threshold shear stress from several papers ranging between 0.002 and 0.7 N m^{-2} for τ_{cd}, and from 0.03 to 1.14 N m^{-2} for τ_{ce}.

In the southwest lagoon of New Caledonia, these parameters and the erosion rate coefficient, ke, are unknown. In the absence of measurements of these parameters, we chose to assume at this stage that τ_{cd} and τ_{ce} are equal to a value hereafter denoted by τ_{cr} (critical shear stress), meaning that there is always either net deposition or net erosion over a given area, except over the reefs where erosion of fine sediments does not occur. We also assumed that the overall fluxes of sediment at the seabed in the lagoon can be considered as zero at a tidal scale for the mean conditions of tide and wind in the absence of river inputs. This assumption implies that:

1. the values of parameters τ_{cr} and ke should provide a balance between deposition and erosion integrated over a tidal cycle, and over the southwest lagoon for mean forcings, and
2. the areas of net deposition obtained in such simulations should be in best agreement with the areas where fine particles are dominant at the seabed. For that comparison, we refer to the distribution of the percentage of mud measured by Debenay (1987), and Chardy et al. (1988; Fig. 5).

Computations were first performed for different values of τ_{cr} combining the tide with mean trade wind of 8 m s^{-1}. Whatever the value of the erosion coefficient ke, increasing values of τ_{cr} lead to greater deposition areas because of the deposition flux formula, and to smaller erosion zones, the area where τ is greater than τ_{cr} being smaller. Tests (Figs. 6c and 7c with $\tau_{cr} = 0.017$ N m^{-2}) showed that values of τ_{cr} equal to 0.015 or 0.017 N m^{-2} lead to erosion and deposition areas in good agreement with the observed distribution of fine particles at the seabed (Fig. 5). The precise value needs to be confirmed through in-situ measurements. The first test runs were performed setting ke_c equal to 5×10^{-5} g m^{-2} s^{-1} which does not have any influence on the erosion and deposition areas. A value of 0.017 N m^{-2} for τ_{cr} was considered to estimate the erosion rate coefficient ke, and we performed a sensitivity study of the model to τ_{cr} varying around 0.017 N m^{-2} once ke_c was tentatively determined.

Determination of a mean value for ke_c

The value of the erosion rate coefficient ke depends essentially on the nature and porosity of the deposit, and may be estimated for each area. As for the critical shear stresses for erosion or deposition, the values cited in the literature are widely scattered. For example, Brenon (1997) quotes values varying between 10^{-5} and 10^{-2} kg m^{-2} s^{-1} in the literature dealing with estuaries.

Under our assumption of equal τ_{cd} and τ_{ce} values, the value of coefficient ke does not modify the type of flux occurring (erosion or deposition) but does affect the quantity of any particulate matter which is eroded – when ke_c is multiplied by a factor of n, erosion is increased by the same factor. The formula for deposition does not change, but the amount of particulate matter deposited increases with increasing ke. Results obtained with tide combined with an averaged wind over the whole lagoon show that values below 10^{-5} g m^{-2} s^{-1} produce erosion fluxes which are insignificant compared to deposition under mean meteorological situations.

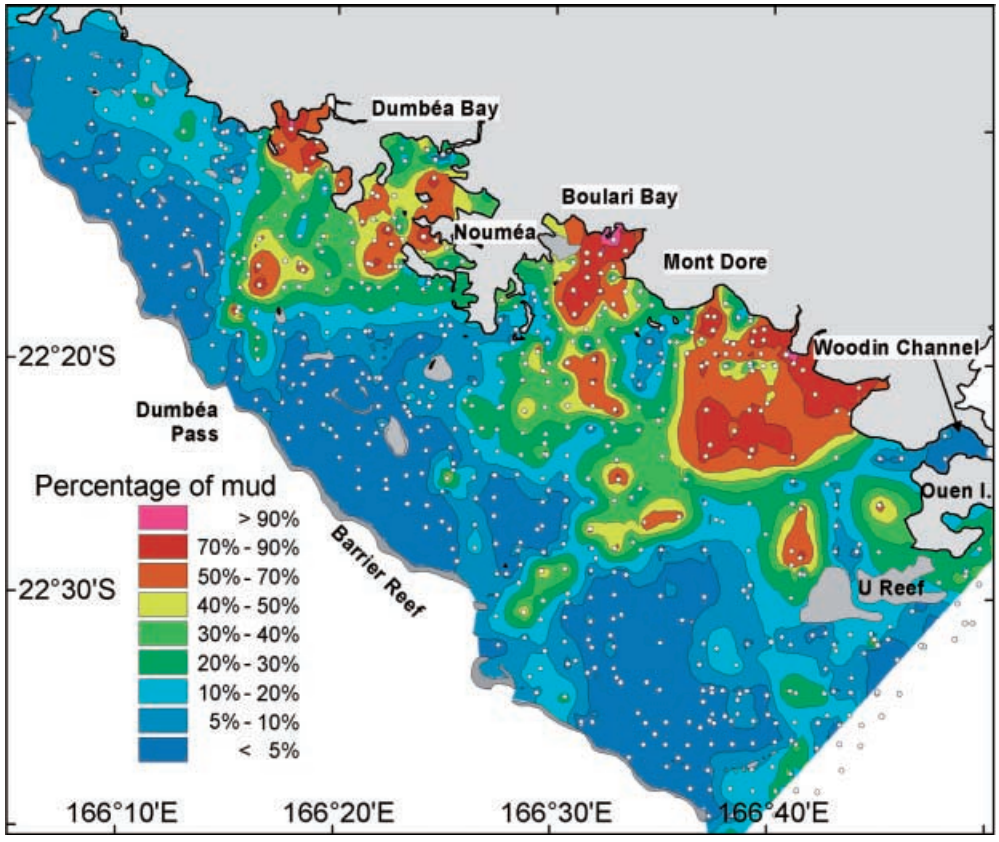

Fig. 5 Distribution of sediment pattern. Isopleth map of mud distribution according to Debenay (1987) and Chardy et al. (1988). *Dots* represent the location of sedimentological samples

Values above 10^{-4} g m^{-2} s^{-1} provide such large erosion fluxes that deposition is necessarily less.

The influence of the coefficient ke_c was studied for values in the range of 4×10^{-5} to 8×10^{-5} g m^{-2} s^{-1}, in the presence of the tide and of several wind conditions. For the sake of comparison, the computed deposition (D_f) and erosion (E_f) fluxes were integrated over the whole lagoon. Their values, summed over a tidal cycle (12.42 h), are expressed in tonnes in Table 1 for a value of 0.017 N m^{-2} for τ_{cr}.

For deposition and erosion integrated over the lagoon to be of the same order of magnitude, for the mean meteorological condition, requires $ke_c = 7.5\times10^{-5}$ g m^{-2} s^{-1}. For this same value of ke_c, the results show that in the absence of wind, the particles settle whereas under combined tide and trade winds of 10 m s^{-1}, particles are eroded. It must be noted that the same equilibrium between erosion and deposition with $\tau_{cr} = 0.015$ N m^{-2} is obtained with $ke_c = 6.0\times10^{-5}$ g m^{-2} s^{-1}. So, several combinations of these parameters are possible (within our assumptions), providing that τ_{cr} is not very different from 0.016 N m^{-2}. The number of possibilities can only be reduced when at least one of these parameters is measured.

Determination of the Schmidt number

Studies have been made of the effect of varying the Schmidt number σ_c. The results show that there is no significant difference between the integrated fluxes of deposition and erosion over the whole lagoon. Erosion does not change, and deposition decreases only slightly (less than 15 over 2,583 to) when σ_c decreases from 1 to 0.5. However, the Schmidt number has a significant influence on the suspended particle profile through the water column. A first comparison of predicted and measured suspended particulate concentration profiles at one marine station in Dumbéa Bay suggested that σ_c about equal to 1 was correct.

Sensitivity of the sediment fluxes to the critical shear stress

The influence of the critical shear stress for deposition and erosion under several wind and tide conditions were studied. Deposition and erosion fluxes were calculated for different values of τ_{cr} in the range 0.010–0.025 N m^{-2} (see Table 2). The coefficient ke_c was considered to be equal to 5×10^{-5} g m^{-2} s^{-1} in these calculations.

For the tide alone, erosion is weak and deposition, which depends on the initial concentration field, is strong. With wind alone, deposition is greater than erosion when τ_{cr} is greater than about 0.012 N m^{-2} for a wind of 8 m s^{-1}, or than about 0.022 N m^{-2} for a wind of 10 N m^{-2}. Considering a combination of the tide and a trade wind of 10 m s^{-1}, erosion increases rapidly when τ_{cr} decreases. In that case, the velocity profile due to the

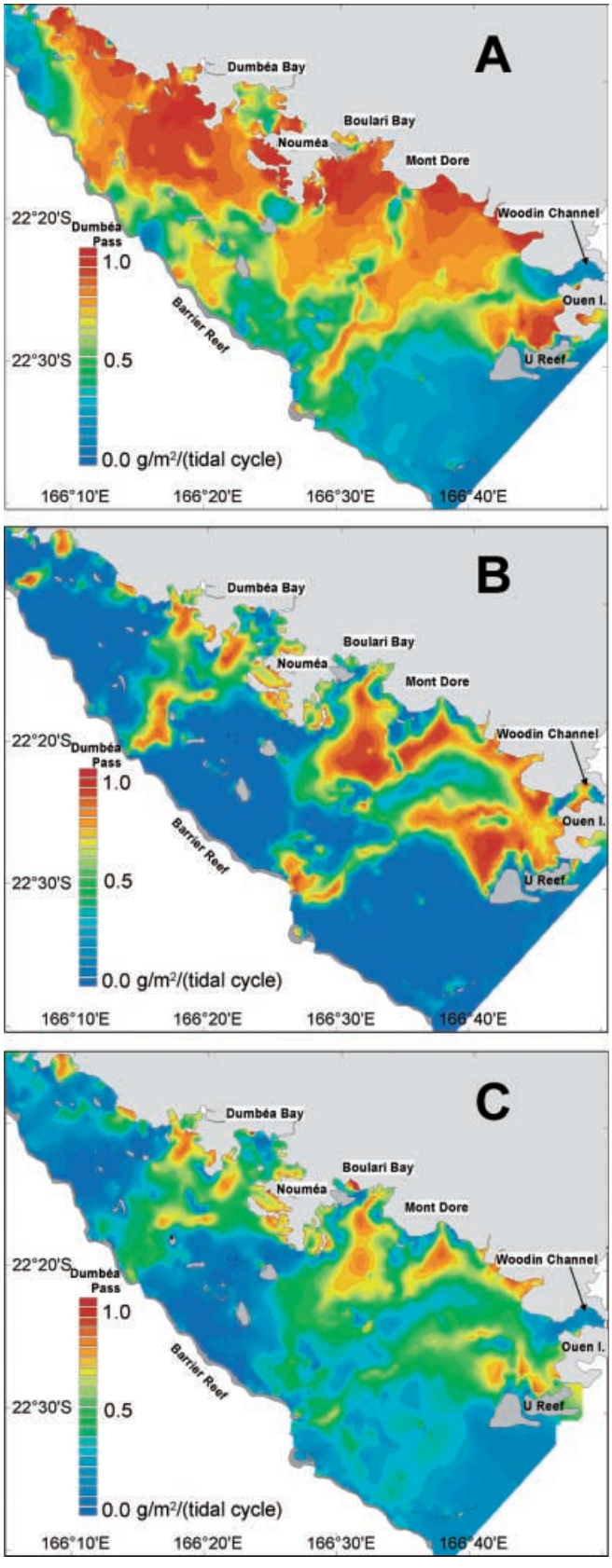

Fig. 6A–C Distribution of deposition flux cumulated over a tidal cycle for different forcings. **A** Tide; **B** trade wind 8 m s^{-1}; **C** tide and trade wind 8 m s^{-1}

combined forcing generates stronger bed shear stresses, and the area where τ is greater than τ_{cr} is greater over a longer period.

Discussion of deposition and erosion for different forcings

The sensitivity studies presented above provide a first determination of the three parameters: the critical shear stresses for deposition and erosion, and the coefficient of erosion. It is instructive to analyze the distribution of deposition and erosion areas calculated for different forcings with $\tau_{cd} = \tau_{ce} = 0.017$ N m^{-2} and $ke_c = 7.5 \times 10^{-5}$ g m^{-2} s^{-1}, as compared to the sediment pattern (Fig. 5). Looking at each process, and comparing the resulting deposition and erosion areas to those obtained with tide and wind combined, should be helpful in identifying the respective role of each process.

Figure 6 presents the charts of the deposition flux cumulated during one tidal cycle for the different forcings: the tide (Fig. 6a), a trade wind of 8 m s^{-1} (Fig. 6b), and the tide combined with a trade wind of 8 m s^{-1} (Fig. 6c). The distribution of the deposition resulting from the combination of tide and trade wind (Fig. 6c) appears to be in good agreement with zones of high percentage of fine particles at the bottom, as is shown in Fig. 5. The deposition is maximum close to the coast, except in a few places such as the south (Woodin Channel), close to Mont Dore, Dumbéa Bay, and in the north. Maximum offshore deposition is observed in the canyons which lead to passes. No deposition areas occur between the barrier reef and Nouméa, and north to Dumbéa Pass. In the model, the tongue of lower deposition in the middle of the lagoon does not appear in the observations of the percentage of mud (Fig. 5). This is partly due to the fact that the wind used in the model is too strong for this part of the lagoon (wind data show a decrease of the wind near the coast, and the variation of wind distribution is not taken into account in the present simulations), and partly to the scarcity of data for the percentage of mud in this area. The distributions of deposition calculated for each forcing alone (Fig. 6a, b) show significant discrepancies with the percentage of mud. They also show the respective influences of the two factors, and demonstrate that the combination of the two forcings is essential to determining the distribution. The tide induces varying current velocities during the tidal cycle, which may be oriented differently from the wind-induced currents. Under the tidal influence, the bed shear stress may alternate between values above and below the critical shear stress threshold for deposition. The tidal influence is greater in the deepest part of the lagoon where the tide operates as the main regulator. The wind is more predominant in shallow areas. The area north to Dumbéa Pass, and the one between the barrier reef and Nouméa, which are shallow and where the percentage of mud is very low, appear as deposition areas when the tide alone is considered.

Table 1 Deposition (D_f) and erosion (E_f) fluxes calculated by the model over the whole lagoon with different values of the coefficient of erosion and with $\tau_{cr} = 0.017$ N m^{-2}. D_f and E_f are expressed in tonnes per tidal cycle

ke_c (g m^{-2} s^{-1})	Wind 8 m s^{-1}	Wind 10 m s^{-1}	Tide	Tide + wind 8 m s^{-1}	Tide + wind 10 m s^{-1}
4×10^{-5}	D_f = 2,369	D_f = 1,445	D_f = 4,805	D_f = 2,625	D_f = 1,664
	E_f = 0797	E_f = 2,148	E_f = 0371	E_f = 1,377	E_f = 2,802
5×10^{-5}	D_f = 2,369	D_f = 1,446	D_f = 4,806	D_f = 2,629	D_f = 1,669
	E_f = 0997	E_f = 2,685	E_f = 0464	E_f = 1,722	E_f = 3,503
6×10^{-5}	D_f = 2,370	D_f = 1,447	D_f = 4,807	D_f = 2,634	D_f = 1,675
	E_f = 1,196	E_f = 3,222	E_f = 0557	E_f = 2,066	E_f = 4,203
7×10^{-5}	D_f = 2,370	D_f = 1,447	D_f = 4,808	D_f = 2,639	D_f = 1,680
	E_f = 1,396	E_f = 3,759	E_f = 0650	E_f = 2,411	E_f = 4,904
7.5×10^{-5}	D_f = 2,371	D_f = 1,448	D_f = 4,808	D_f = 2,641	D_f = 1,683
	E_f = 1,495	E_f = 4,028	E_f = 0696	E_f = 2,583	E_f = 5,254
8×10^{-5}	D_f = 2,373	D_f = 1,448	D_f = 4,809	D_f = 2,643	D_f = 1,686
	E_f = 1,595	E_f = 4,296	E_f = 0743	E_f = 2,755	E_f = 5,605

Table 2 Deposition (D_f) and erosion (E_f) fluxes calculated by the model over the whole lagoon with different values of the critical shear stress and with $ke_c = 5\times10^{-5}$ g m^{-2} s^{-1}. D_f and E_f are expressed in tonnes per tidal cycle

$\tau_{cd} = \tau_{ce}$ (N m^{-2})	Wind 8 m s^{-1}	Wind 10 m s^{-1}	Tide	Tide + wind 8 m s^{-1}	Tide + wind 10 m s^{-1}
	D_f = 2,997	D_f = 1,993	D_f = 5,378	D_f = 3,252	D_f = 2,213
0.025	E_f = 0499	E_f = 1,474	E_f = 0258	E_f = 0952	E_f = 1,984
	D_f = 2,636	D_f = 1,662	D_f = 5,057	D_f = 2,889	D_f = 1,889
0.020	E_f = 0755	E_f = 2,187	E_f = 0364	E_f = 1,344	E_f = 2,768
	D_f = 2,369	D_f = 1,446	D_f = 4,806	D_f = 2,629	D_f = 1,669
0.017	E_f = 0997	E_f = 2,685	E_f = 0464	E_f = 1,722	E_f = 3,503
	D_f = 2,165	D_f = 1,296	D_f = 4,604	D_f = 2,434	D_f = 1,510
0.015	E_f = 1,224	E_f = 3,251	E_f = 0559	E_f = 2,077	E_f = 4,181
	D_f = 1,554	D_f = 0890	D_f = 3,924	D_f = 1,844	D_f = 1,064
0.010	E_f = 2,332	E_f = 5,850	E_f = 1,010	E_f = 3,737	E_f = 7,240

Figure 7 presents the maps of erosion fluxes cumulated over a tidal cycle for the same forcings as in Fig. 6: the tide (Fig. 7a), a trade wind of 8 m s^{-1} (Fig. 7b), and the tide combined with a trade wind of 8 m s^{-1} (Fig. 7c). From a physical point of view, erosion is supposed to occur preferably over the areas where the percentage of coarse particles at the bottom is greatest, whereas bottoms dominated by fine particles represent favorable areas of deposition. Indeed, the combination of tide and wind (Fig. 7c) provides the best agreement between simulations and the distribution of mud at the bottom. For the tide alone (Fig. 7b), the erosion areas are limited to the south of the lagoon and Woodin Channel. For the wind alone (Fig. 7a), the erosion areas are much larger but they are confined to the shallow waters. In the two latter cases, the bed shear stress is generally lower than the critical shear stress for erosion. As expected, the wind effect at the bottom is predominant in the shallower part of the lagoon and its influence over the deepest areas is weak. For example, in Woodin Channel (>20 m deep), there is no erosion when the wind alone is considered, whereas erosion is maximum when combining tidal forces. It appears that the wind has no significant effect in the exchange process at the bottom when the water depth is greater than about 20 m. Beyond this depth, the tide has a greater influence in the transport of the suspended particulate matter and seems to determine the redistribution of the particles in the lagoon.

Conclusion

The work presented in this paper forms part of the ECOTROPE and PNEC programs, which study the influence of anthropogenic and terrigenous inputs on the southwest lagoon of New Caledonia. A numerical model of the transport of fine suspended particulate matter was developed and tested. Calibration and sensitivity tests were carried out to obtain a first evaluation of the mean parameters involved in the sedimentary processes through the water column and at the sediment-water interface. Values of the critical shear stress for deposition and erosion, as well as the erosion rate coefficient were estimated over the whole southwest lagoon of New Caledonia, for a characteristic fine sediment. The calibration relies on the distribution of the percentage of mud reported by Debenay (1987) and Chardy et al. (1988), and uses the assumption that the erosion and deposition fluxes integrated over a tidal cycle should be of the same order of magnitude for a typical trade wind of 8 m s^{-1} combined with the tide. Very good agreement between the simulated distribution and the measurements was obtained when critical shear stresses

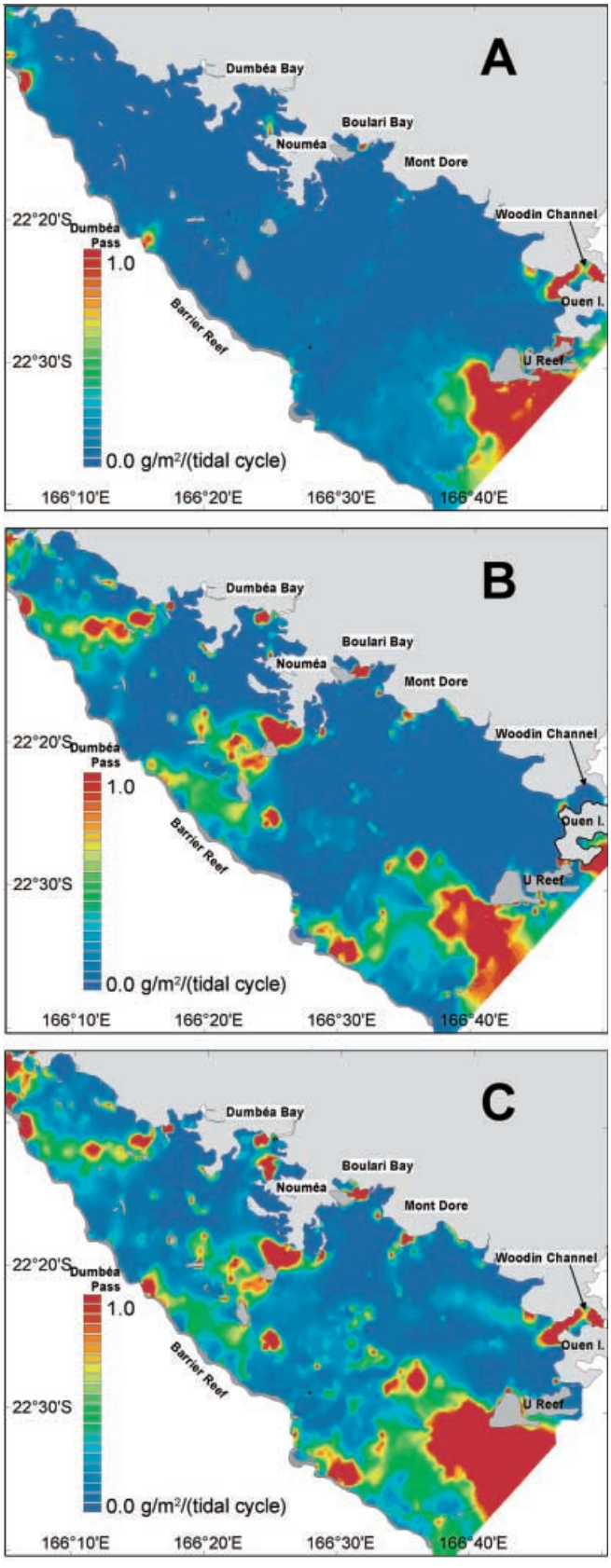

Fig. 7A–C Distribution of erosion flux cumulated over a tidal cycle for different forcings. **A** Tide; **B** trade wind 8 m s^{-1}; **C** tide and trade wind 8 m s^{-1}

for erosion and deposition were set at 0.017 N m^{-2}, and an erosion rate coefficient of 7.5×10^{-5} g m^{-2} s^{-1} was chosen. Two important points were highlighted:

1. The influence of wind is predominant in the processes of deposition and erosion in the shallow areas, with a most direct influence on erosion when the depth is less than 20 m;
2. The tide, which is a permanent process, largely controls the particulate transport, the vertical mixing in the water column, and finally the deposition in the areas where the influence of the wind is weak.

This study principally examined the calibration of the model of suspended particulate matter transport through the fluxes of particles at the bottom, but the resulting parameters need to be confirmed by in-situ measurements. Future numerical studies will focus on the distribution of the suspended particulate matter in the water column. The influence of vertical eddy diffusivity will be further studied through a comparison with more complex turbulent models, and a study of the Schmidt number documented by more depth profiles of suspended sediment concentration. A distribution of particles with different diameters could also be introduced into the model. The waves generated by the local wind also have an influence on deposition and erosion in the shallower parts of the lagoon which should be introduced into the model. The model could then tentatively be used for simulating heavy rainfall conditions, and a comparison be conducted with satellite data when available, airborne data, and in-situ measurements of turbidity.

Acknowledgments This work was supported by the Institut de Recherche pour le Développement (Ecotrope – UR CAMELIA) and by the French Programme National Environnement Côtier.

References

Blumberg AF, Mellor GL (1987) A description of the three-dimensional coastal ocean circulation model. In: Heaps NS (ed) Three-dimensional coastal ocean model. Am Geophys Union, Washington, DC, pp 1–16

Brenon I (1997) Modélisation de la dynamique des sédiments fins dans l'estuaire de la Seine. PhD Thesis, University Bretagne Occidentale

Brenon I, Le Hir P (1999) Modelling the turbidity maximum in the Seine estuary (France): Identification of formation processes. Estuarine Coastal Shelf Sci 49:525–544

Celik I, Rodi W (1988) Modelling suspended sediment transport in nonequilibrium situations. J Hydraulic Eng 114:1613–1641

Chapalain G, Thais L (2000) Tide, turbulence and suspended sediment modelling in the eastern English Channel. Coast Eng 41:295–316

Chardy P, Chevillon C, Clavier J (1988) Major benthic communities of the south-west lagoon of New Caledonia. Coral Reefs 7:69–75

Coleman NL (1970) Flume studies of the sediment transport coefficient. Water Resources Research 6:3

Debenay JP (1987) Sedimentology in the South-West Lagoon of New-Caledonia, SW Pacific. J Coast Res 3:77–91

Deleersnijder E, Beckers JM (1992) On the use of the σ-coordinate system in regions of large bathymetric variations. J Mar Syst 3:381–390

Douillet P (1998) Tidal dynamics of the south-west lagoon of New Caledonia: observations and 2D numerical modelling. Oceanol Acta 21:69–79

Douillet P, Bargibant G, Hoffchir C, Laboute P, Menou JL, Panché JY, Tirard P (1989) Mesures de courant, de marée et de vent dans le lagon sud-ouest de Nouvelle Calédonie. 1ère partie: octobre 1988 à juillet 1989. Rapp Sci Tech ORSTOM Nouméa, Sci Mer, Biol Mar 53

Douillet P, Bargibant G, Hamel P, Hoffschir C, Menou JL, Panché JY, Tirard P (1990) Mesures de courant, de marée et de vent dans le lagon sud-ouest de Nouvelle-Calédonie. 2ème partie: juillet 1989 à octobre 1990. Rapp Sci Tech ORSTOM Nouméa, Sci Mer, Biol Mar 58

Durand N, Fiandrino A, Fraunié P, Ouillon S, Forget P, Naudin JJ (2001) Suspended matter dispersion in the Ebro ROFI: an integrated approach. Cont Shelf Res (in press)

Frith CA, Mason LB (1986) Modelling wind driven circulation One Tree Reef, Southern Great Barrier Reef. Coral Reefs 4:201–211

Hearn CJ, Holloway PE (1990) A three dimensional barotropic model of the response of the Australian North West Shelf to tropical cyclones. J Phys Oceanogr 20:60–80

Jarrige F, Radok R, Krause G, Rual P (1975) Courants dans le lagon de Nouméa (Nouvelle Calédonie). Déc. 74–janv. 75. Rapp ORSTOM (Nouméa) and H Lamb Inst Oceanogr, Flinders University, S Australia

Kraines SB, Yanagi T, Isobe M, Komiyama H (1998) Wind-wave driven circulation on the coral reef at Bora Bay, Miyako Island. Coral Reefs 17:133–143

Krone RB (1962) Flume studies of the transport of sediment in estuarial shoaling processes. Tech Rep Hydraulic Eng Lab and Sanitary Eng Res Lab, University California, Berkeley, CA

Lazure P, Salomon JC (1991) Coupled 2-D and 3-D modelling of coastal hydrodynamics. Oceanol Acta 14:173–180

Leendertse JJ (1967) Aspects of a computational model for long-period water-wave propagation. The Rand Corporation, Santa Monica, CA, Rep RM-5294-PR

Le Normant C (1995) Modélisation numérique tridimensionnelle des processus de transport des sédiments cohésifs en environnement estuarien. PhD Thesis, Inst Natl Polytech Toulouse

Lin BL, Falconer RA (1996) Numerical modelling of three-dimensional suspended sediment for estuarine and coastal waters. J Hydraulic Res 34:435–456

Mehta AJ, Hayter EJ, Parker WR, Krone RB, Teeter AM (1989) Cohesive sediment transport I: Process description. J Hydraulic Eng 115:1076–1093

Morlière A (1985) Assainissement de Nouméa. Mesures de courant. Rapp Sci Tech ORSTOM

Morlière A, Crémoux JL (1981) Observations de courant dans le lagon, de février à août 1981. Rapp Sci Tech ORSTOM

Nicholson J, O'Connor BA (1986) Cohesive sediment transport model. J Hydraulic Eng 112:621–640

Nihoul JCJ (1984) A three-dimensional general marine circulation model in a remote sensing perspective. Ann Geophys 2:433–442

O'Callaghan J (1999) The oceanography and sedimentology of a coastal embayment: Dumbea Bay, Noumea, New Caledonia. BSc Degree, School of Earth Sciences, James Cook University, S Australia

Ouillon S, Le Guennec B (1996) Modélisation du transport de matières en suspension non-cohésives dans les écoulements 2D verticaux à surface libre. J Hydraulic Res 34:219–236

Partheniades E (1965) Erosion and deposition of cohesive soils. J Hydraulics Div 91:105–139

Piedra-Cueva I, Mory M, Temperville A (1997) A race-track recirculating flume for cohesive sediment research. J Hydraulic Res 35:377–396

Prager EJ (1991) Numerical simulation of circulation in a Caribbean-type backreef lagoon. Coral Reefs 10:177–182

Ruddick KG, Deleersnijder E, Luyten PJ, Ozer J (1995) Haline stratification in the Rhine-Meuse plume: a three-dimensional model sensitivity analysis. Cont Shelf Res 15:1597–1630

Schaaff E (1999) Remise en suspension des sédiments du Golfe du Lion: expériences et modélisation. DEA Sci Env Mar, Université Méditerranée, Marseille

Smith NP (1985) The decomposition and simulation of the longitudinal circulation in a coastal lagoon. Estuarine Coastal Shelf Sci 21:623–632

Soulsby R (1998) Dynamics of marine sands. Thomas Telford, London

Tartinville B, Deleersnijder E, Rancher J (1997) The water residence time in the Mururoa atoll lagoon: sensitivity analysis of a three-dimensional model. Coral Reefs 16:193–203

Teisson C (1991) Cohesive suspended sediment transport: feasibility and limitations of numerical modelling. J Hydraulic Res 29:755–769

Teisson C, Ockenden M, Le Hir P, Kranenburg C, Hamm L (1993) Cohesive sediment transport processes. Coast Eng 21:129–162

van Rijn LC (1986) Mathematical modelling of suspended sediment in non-uniform flows. J Hydraulic Eng 112:433–455

van Rijn LC, van Rossum H, Termes P (1990) Field verification of 2-D and 3-D suspended sediment models. J Hydraulic Eng 116:1270–1288